AGU PUBLICATIONS

JGR

Journal of Geophysical Research: Solid Earth

RESEARCH ARTICLE
10.1002/2014JB011635

This article is a companion to *Nespoli et al.* [2015] doi:10.1002/2014JB011636.

Key Points:
- Anomalous high soil temperatures were measured at the Terre Calde di Medolla
- A CO_2 and CH_4 isotopic decoupling was observed at 0.6 m depth
- Exothermic, oxidative CH_4 removal is the main mechanism of soil heating at TCM

Correspondence to:
B. Capaccioni,
bruno.capaccioni@unibo.it

Citation:
Capaccioni, B., F. Tassi, S. Cremonini, A. Sciarra, and O. Vaselli (2015), Ground heating and methane oxidation processes at shallow depth in Terre Calde di Medolla (Italy): Observations and conceptual model, *J. Geophys. Res. Solid Earth*, *120*, 3048–3064, doi:10.1002/2014JB011635.

Received 23 SEP 2014
Accepted 11 MAR 2015
Accepted article online 21 APR 2015
Published online 19 MAY 2015

Ground heating and methane oxidation processes at shallow depth in Terre Calde di Medolla (Italy): Observations and conceptual model

Bruno Capaccioni[1], Franco Tassi[2,3], Stefano Cremonini[1], Alessandra Sciarra[4], and Orlando Vaselli[2,3]

[1]Department of Biological, Geological and Environmental Sciences, University of Bologna, Bologna, Italy, [2]Department of Earth Sciences, University of Florence, Florence, Italy, [3]CNR-IGG Institute of Geosciences and Earth Resources, Florence, Italy, [4]Istituto Nazionale di Geofisica e Vulcanologia, Rome, Italy

Abstract The toponym "Terre Calde di Medolla" (literally, "Warm Earths of Medolla") refers to a farming area, located near the town of Modena (Emilia-Romagna region, northern Italy), which has always been known by the local population for the relatively high temperatures of the soil. This phenomenon is particularly evident in wintertime when the snow cover over this area rapidly melts. A detailed investigation, carried out after the devastating 2012 Emilia earthquake that affected this area, showed soil temperatures up to 44°C, i.e., 20–25°C above the local background value, together with diffuse soil fluxes of CH_4 (0–2432 $g \times m^{-2} \times d^{-1}$) and minor, though significant, CO_2 (0–1184 $g \times m^{-2} \times d^{-1}$), especially from subcircular (a few meters in diameter) zones. Ground heating and gas seepage appear spatially correlated, thus suggesting a close relationship between the two phenomena. The anomalous high ground temperature is not associated with an anomalous geothermal gradient or with the uprising of deep-seated hot fluids. According to the lateral and vertical distributions of the temperatures as well as the chemical and isotopic compositions of the soil gases, the most reliable explanation is the exothermic oxidation of diffusely uprising biogenic methane at very shallow levels (<1 m). Such a process occurs in the presence of free oxygen and methanotrophic bacteria and can then explain (i) the observed ground heating up, (ii) the diffuse emission from the soil of CO_2 characterized by an extremely negative isotopic ($^{13}C/^{12}C$) signature, and (iii) the lack of diffuse and low CH_4 fluxes. According to these hypotheses, the heating phenomena affecting the shallow groundwater and the ground surface, as described by several witnesses in the area of the May–June 2012 Emilia earthquake, could be related to either a coseismic or postseismic onset of new areas affected by CH_4 seepage or an increase in preexisting CH_4 fluxes.

1. Introduction

Methane, in spite of its relatively low, though growing, concentration in air (about 1800 ppbv [*Kirschke et al.*, 2013, and references therein]), poses a severe environmental concern, since its global warming potential is 25 CO_2-eq in a 100 year time horizon [*Cicerone and Oremland*, 1988; *Hansen et al.*, 1998]. The origin of CH_4 in the atmosphere is related to different anthropogenic (e.g., rice paddies, livestock farms, biomass burning, oil and gas mining, and waste disposal) and natural (e.g., wetlands, termites, oceans, freshwaters, and seepage from deep reservoirs in both sedimentary and volcanic environments) sources. Gas seepage from geological sources has traditionally not been considered important [*Lelieveld et al.*, 1998]. Nevertheless, sedimentary basins account for 90% [*Etiope and Klusman*, 2002] of the total geogenic CH_4, while those associated with geothermal and volcanic sources are less than 10% [*Etiope et al.*, 2007]. In faulted areas, CH_4 diffuse seepage from the ground may reach hundreds of $mg \times m^{-2} \times d^{-1}$ [*Etiope*, 2009], preventing biogeochemical oxidation processes in the soil to completely consume this gas uprising from depth.

The "Terre Calde di Medolla" (literally, the Warm Earths of Medolla, hereafter TCM) is a toponym used in a farming area of less than 1 km^2 located close to Medolla (Figures 1a–1c), a small municipality in the Province of Modena (approximately 45 km NW of Bologna, northern Italy). In this area, the occurrence of several small subcircular (<10 m in diameter) zones, characterized by anomalously high ground temperature ("*warm Earth*") and clearly noticeable during wintertime as the snow cover quickly melts, has been known at least since the late nineteenth century [*Spinelli*, 1893; *Spinelli and Cuoghi Costantini*, 1893;

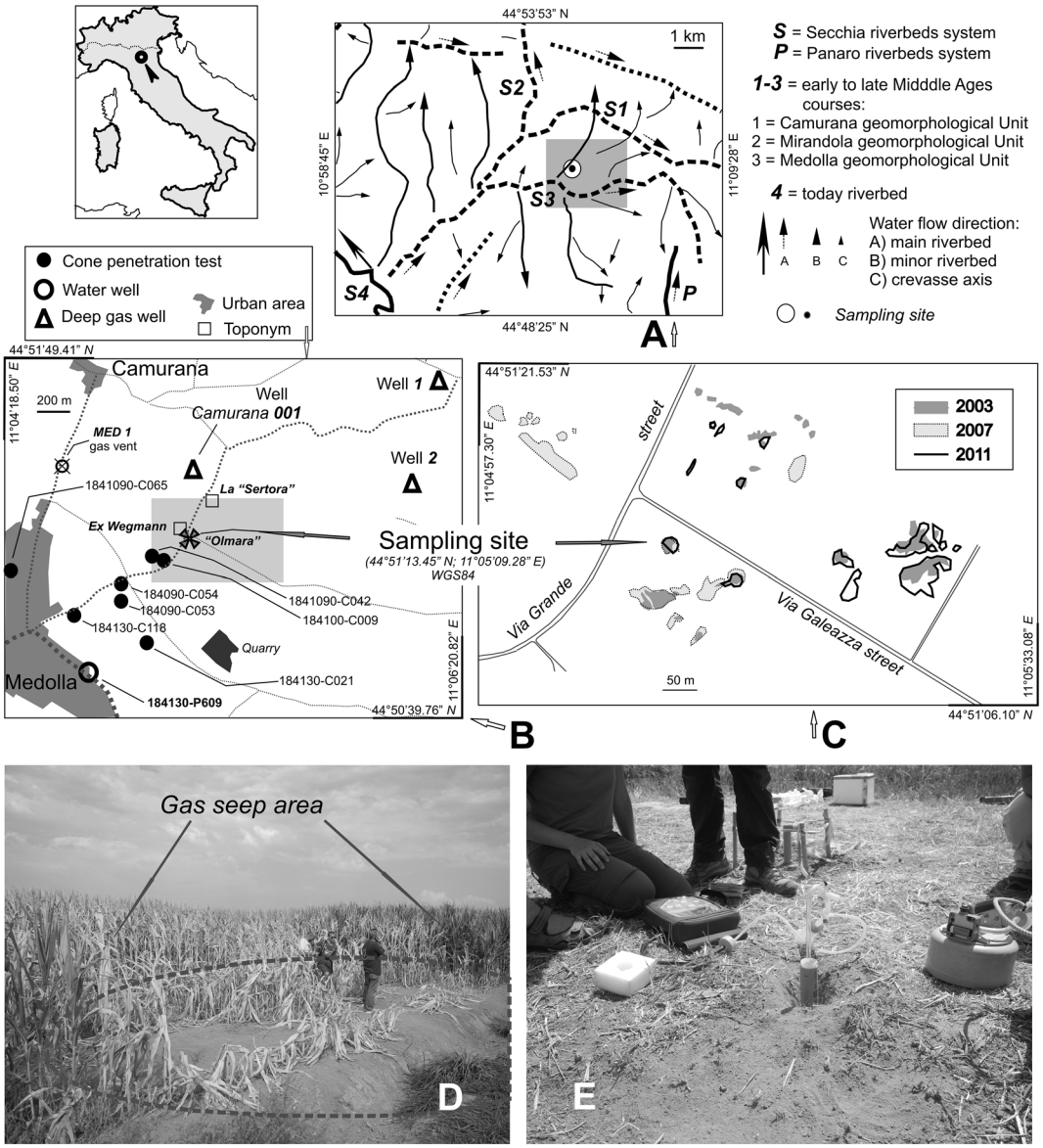

Figure 1. Locational settings of the study area. (a) Paleo-riverbeds of the Secchia River in the Medolla area. (b) Location of the various boreholes and CPTs used to draw the stratigraphic log of Figure 2b: the numerical codes are referring to that figure. The location of the MED 1 gas emission is reported. (c) Planform of the vegetation anomalies due to the natural gas seep around the sampling site: The boundaries were outlined from satellite imagery (Google©) at various years after 2007. (d) The aspect of the sampled main gas seep site: The seeping area extends beyond the agrarian ditch on the lower right corner. (e) Gas sampling phase at the study site.

Gasperi and Pellegrini, 1981]. Anomalous and occasionally abrupt temperature increases (up to 50–60°C) have also been reported to repeatedly occur in the shallow groundwater, such as recorded after the May–June 2012 Emilia seismic sequence that caused 27 fatalities and strong damages to residential dwellings, infrastructures, and local economy [e.g., *Anzidei et al.*, 2012; *Govoni et al.*, 2014]. The TCM area shows macroseeps; e.g., mud volcanoes [e.g., *Tassi et al.*, 2012, and references therein]; microseepage, i.e., anomalously high soil CH_4 and, at a lesser extent, CO_2 fluxes [*Sciarra et al.*, 2012, 2013]; and fossil wax (*ozocherite*) [*Spinelli*, 1893; *Spinelli and Cuoghi Costantini*, 1893]. The presence of these manifestations (Figure 1c) at the surface seriously affects the growth of some cultivated areas (Indian corn; Figure 1d). According to the description reported by *Spinelli* [1893] and *Spinelli and Cuoghi Costantini* [1893], the location of these gas seepages has remained relatively stable at least over the past 120 years.

The peculiar features of TCM, described and discussed in the present paper, represent an outstanding association between gas microseepage and soil heating, allowing us to (i) evaluate the amount of CH_4 released from this site, (ii) assess the geochemical relationships between CH_4 and CO_2, and (iii) understand the processes that favor the presence of anomalous temperature at the surface.

2. Geological Background

2.1. Geomorphological Setting

TCM is located (World Geodetic System 84: 44°51′13.45″N, 11°05′09.28″E) in the middle of the Po River plain (Figure 1), at an elevation of 21 m above sea level. It lies at the intersection of a number of alluvial ridges generated by the Secchia River paleochannels (Figure 1a). The whole domain of the Secchia alluvial ridges progressively covered the anabranching Po River alluvial plain [*Cremonini*, 2007; *Bianchini et al*., 2014], which is characterized by sandy paleomeanders still out cropping a few kilometers northward.

2.2. Structural Setting

The northern Apennine orogenic front (Figure 2a) is composed of two geographic domains, i.e., an emerged (Apennine Chain in a strict sense) and outermost (*Dorsale Ferrarese*) part, buried beneath the Po River alluvial plain, located at about 50 km northward from the foothill chain [*Consiglio Nazionale delle Ricerche* (*CNR*), 1990; *Cerrina Feroni et al*., 2002; *Boccaletti and Martelli*, 2004]. In particular, the *Cavone-Mirandola* thrust (Figure 2d) was the first anticline structure of the buried front to be generated in the outermost domain [*Ghielmi et al*., 2010]. The double chain front is likely still active in response to the general compressive stress field [*Michetti et al*., 2012] dating from the middle Pleistocene. This buried front is still undergoing a synsedimentary growth according to a decreasing rate of the tectonic uplift from 0.53 to 0.16 mm/yr during the last 1.4 Myr [*Scrocca et al*., 2007; *Picotti and Pazzaglia*, 2008]. Owing to this growth, the top of the buried *Dorsale Ferrarese* tectonic folds in the area near Medolla and Mirandola, as well as near Ferrara (Figure 2a), lies at a very shallow depth beneath the alluvial plain, often less than 100 m [*CNR*, 1990].

The up-to-date activity of this sector of the buried Apennine front was confirmed by the May 2012 Emilia seismic sequence [*Galli et al*., 2012; *Ventura and Di Giovambattista*, 2013; *Cesca et al*., 2013]. During this seismic sequence, the vertical component of the deformation attained a relative maximum (112 mm) at the study site [*Borgatti et al*., 2012; *Galli et al*., 2012].

The schematic cross section in Figure 2d [*International Commission on Hydrocarbon Exploration and Seismicity in the Emilia Region* (*ICHESE*), 2014] intimately resembles the geological setting of the *Cavone-Mirandola* structural high [*Nardon et al*., 1991; *Carminati et al*., 2010].

2.3. Stratigraphic Setting

The stratigraphic details recorded in the surficial domain (Figure 3a) consist of proximal to median crevasse deposits related to the main paleo-Secchia *Unit of Medolla* and its younger geomorphologic subunits. The homogeneous grey-greenish color of the superficial layers is to be considered as a specific feature of the study area from where gas seepage occurs.

A medium-depth stratigraphic sequence (Figure 3b) has been obtained by merging stratigraphic data available within 1 km distance of the investigated area (Figure 1b). The prominent feature is the existence of two sandy river-channel facies, which can be referred to the Po riverbed due to both their thickness (14 m) and homogeneity. According to available data in the surrounding areas [*Cremonini*, 1993; *Amorosi et al*., 2008], the whole sequence likely represents the entire Last Glacial period (Weichselian/Würmian: oxygen isotope stages (OISs) 2–5) up to a depth of 60 m. According to the stratigraphic model proposed by *Amorosi and Colalongo* [2005], the peaty clay layer lying at 61 m depth (Figure 3c) represents the most internal transgressive system tract deposits correlated with the maximum flooding surface of the Last Interglacial period (Eeemian: OIS 5e). This would confirm its location as far as more than 60 km westward with respect to the homologue Holocene facies [*Amorosi et al*., 2000]. The 33 m thick bank of sandy clay at 79–113 m in depth is the upper middle Pleistocene slope-shelfal-coastal deposit of the *Ravenna Formation* (*Prograding Complex*, after *Ghielmi et al*. [2010]). The lowermost 10 m of stiff clayey sequence can be regarded as the upper, eroded top of the marine Pliocene *Porto Garibaldi* Formation [*Dondi et al*., 1982;

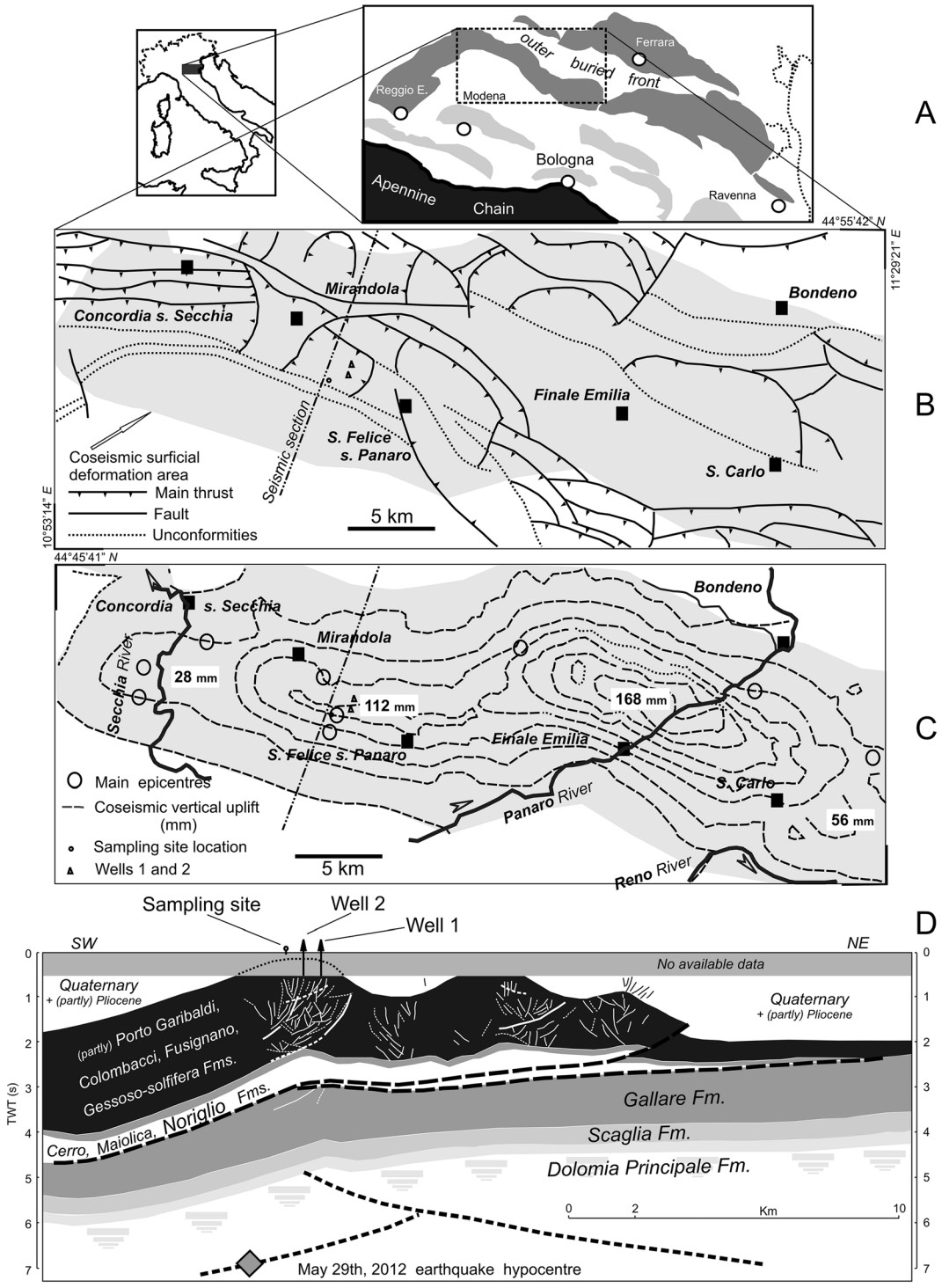

Figure 2. General tectonic setting of the Medolla area. (a) Main thrusts top of the buried Apennine Chain front (*Dorsale Ferrarese* and *Pieghe Romagnole*) and the emerged chain front in the Emilia Po Plain sector. (b) Detail of the *Dorsale Ferrarese* tectonic structures in the epicentral area of the 2012 May seismic sequence: The surficial deformation area is in grey tone (as in Figure 2c). The location of Well 1 and Well 2 of Figure 3 (black triangle) and of the sampling site (black circle) is also shown. (c) Total uplift of the May 2012 earthquake in the epicentral area (after *Borgatti et al.* [2012], redrawn) and main shock epicenter location. (d) Interpretation of the seismic line MOD-74-19 (after *ICHESE* [2014], Figure 7m: redrawn and modified). The projected location of Wells 1 and 2 was derived from Figure 1b. Possible minor faults (mainly, the white lines) are proposed.

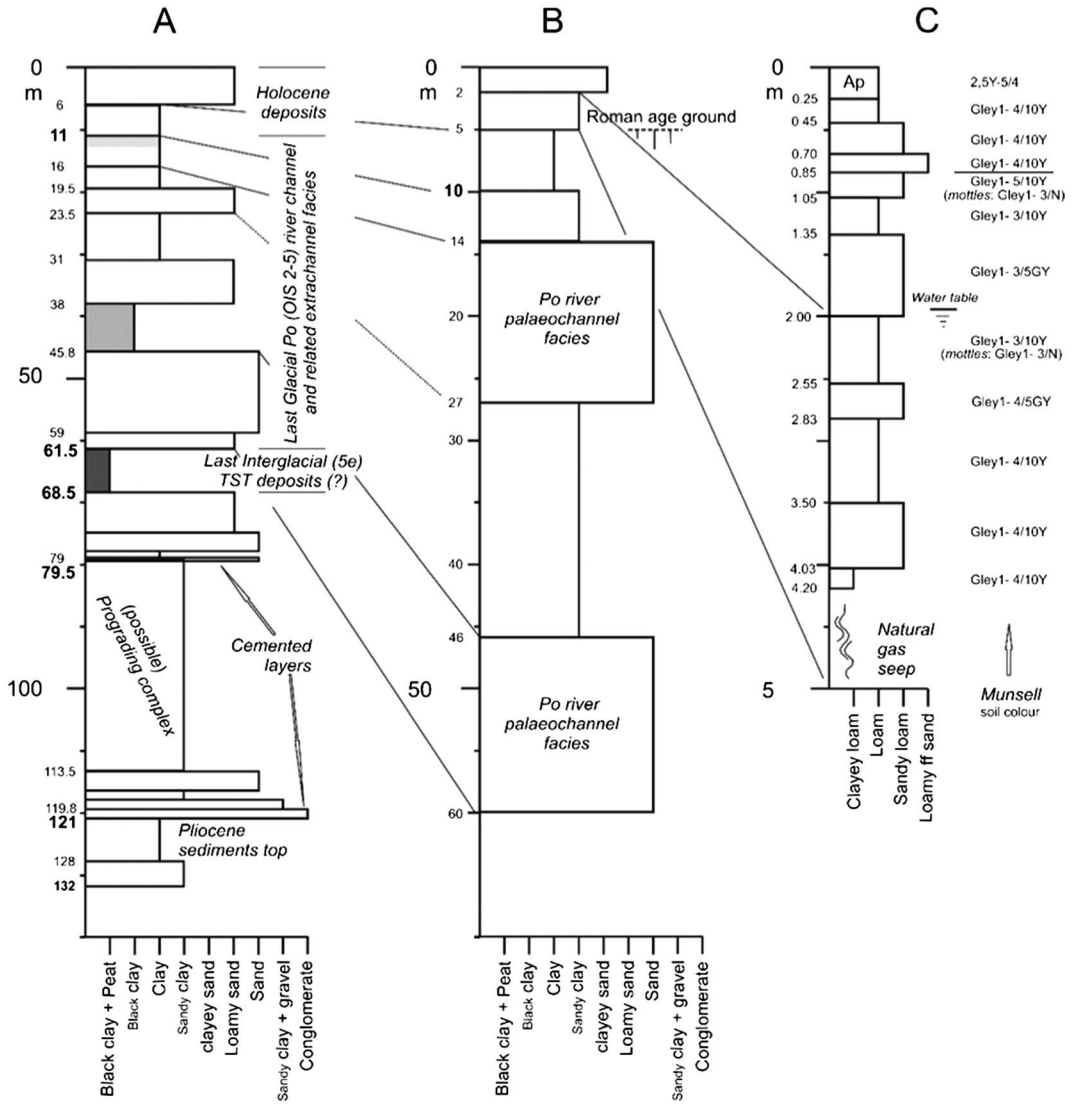

Figure 3. Stratigraphic logs at various depth scales available for the study site area. (a) Textural log from the handmade borehole used for sampling the natural gas seep: The Munsell soil color codes are also provided on the right. (b) Cumulative medium-depth stratigraphic log reconstructed from eight different points available near the sampling site. The single-log original codes (available at the same website of Figure 3a) are listed in Figure 1b. (c) Log of the well Region ER. 184130-P609 redrawn and simplified (available online at https://applicazioni.regione.emilia-romagna.it/cartografia_sgss/user/viewer.jsp?service=sezioni_geo).

Barchi et al., 2001; *Fantoni and Franciosi*, 2010; *Ghielmi et al*., 2010]. Well 1 (Figure 4) indeed shows a very thin layer (only 220 m) of Pliocene sediments due to the tectonic uplift of the *Dorsale Ferrarese* thrust system. The tectonic factor is further stressed by the existence of three to four reverse fault planes lying between 2000 and 2700 m (Figure 4). They are horizontal and consistent with the intense faulting linked to the tectonic thrust setting shown in Figure 2d. Brackish/salt water and CH_4-rich gas are mainly concentrated below the main fault planes, while no gas pockets or anomalous gas enrichments were recorded above them. The Well *Camurana 001* (Figure 1b), drilled 600 m north of the sampling point in 1943 and exploited for about 1 year, recorded a strong gas flow at 741–742 m and gas and slight mineral oil at 904–906 m in depth (http://unmig.sviluppoeconomico.gov.it/videpi/pozzi/consultabili.asp.). Furthermore, between 964 and 1113 m, the shale was described as "*splintery* (and) *highly broken and slickensided*," thus suggesting the possible existence of a noticeable subvertical fault plane, as shown in Figure 2d.

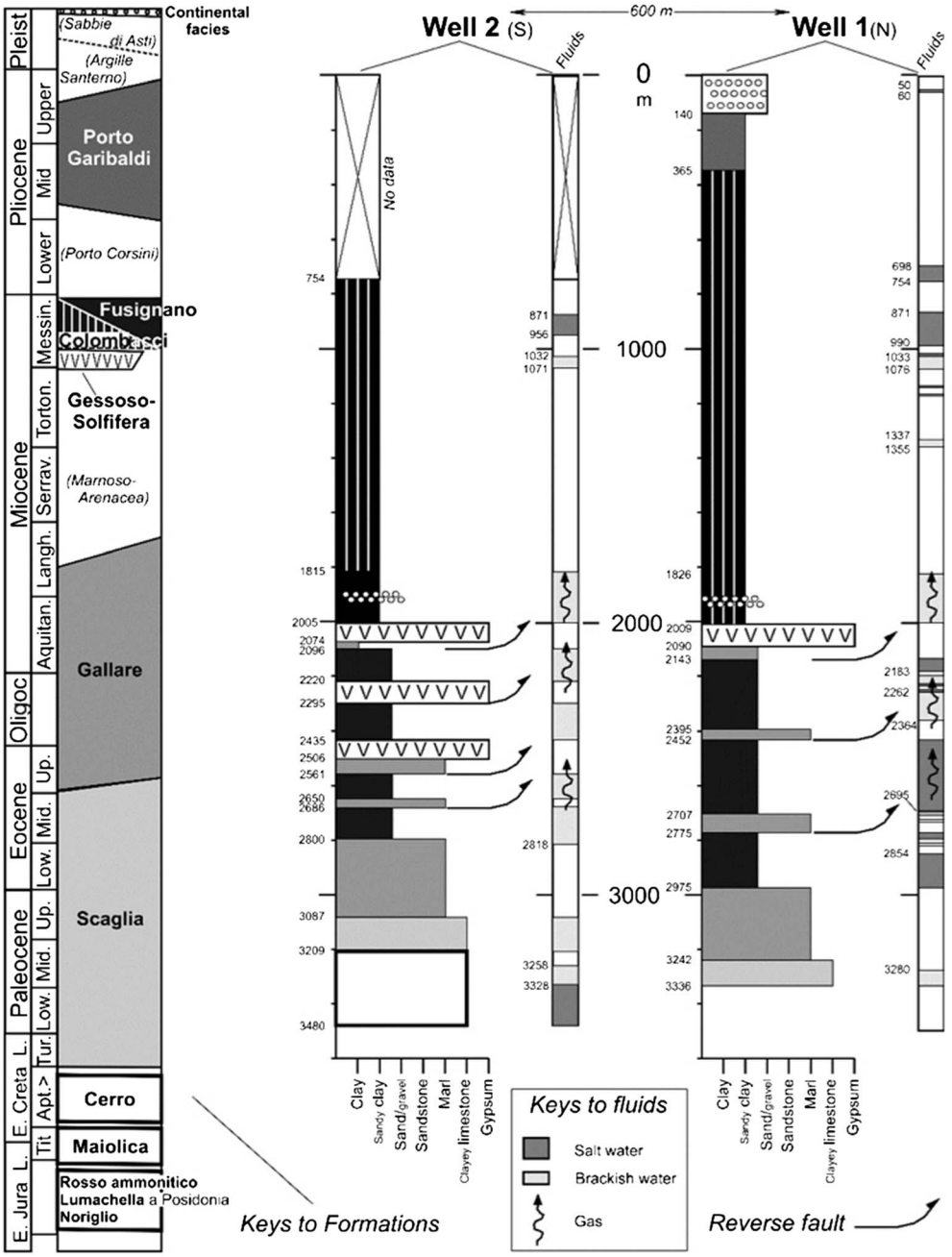

Figure 4. Stratigraphic log of two wells located 1.5 km NE of the study site. Each column was redrawn and simplified: The log Well 1 is available online at the website http://unmig.sviluppoeconomico.gov.it/deposito/pozzi/log/pdf/bignardi_001.pdf; the log Well 2 is available online at the website: http://unmig.sviluppoeconomico.gov.it/deposito/pozzi/log/pdf/bignardi_001_dir_bis.pdf The first column on the left is the general stratigraphic scheme for the central Po River plain subsoil [*Dondi et al.*, 1982] adopted for defining the formation names adopted in the well's log: The formation names in brackets are lacking in the studied area.

3. Materials and Methods

Diffuse CO_2 and CH_4 soil fluxes (microseepage) were measured in the TCM area in July 2008 (50 sites) and July 2013 (138 sites). During these two field campaigns, an area of ~260,000 m^2 was investigated. Gas flux measurements were based on the accumulation chamber "time 0" method [*Norman et al.*, 1992, 1997; *Chiodini et al.*, 1996, 1998, 2000; *Rogie et al.*, 2000; *Brombach et al.*, 2001; *Cardellini et al.*, 2003]. The instrument used was a West System™ portable flux meter, equipped with two infrared spectrophotometer

detectors: (i) Licor 8002 for CO_2 and (ii) tunable laser diode with multipass cell for CH_4. During the 2013 campaign at the same sites, soil temperatures were also recorded at 10 cm depth with a digital thermometer equipped with a 20 cm long PT100 thermocouple.

A 2.5 m deep piezometer was drilled in the SW sector of the investigated area (Figures 1c and 1e), where an anomalously high CO_2 soil flux was measured (up to 103.4 $g \times m^{-2} \times d^{-1}$). During drilling, soil temperatures, CH_4, and CO_2 fluxes as well as collection of gas samples for chemical and isotopic analyses were determined at intervals of 10 cm up to 80 cm depth and at intervals of 50 cm at greater depth. Flux measurements and collection of gas samples were carried out once a plastic tube (4.2 cm in diameter) was positioned in the hole and the internal volume was purged for 2′. A certain degree of uncertainty (±5 cm, i.e., the length of the core barrel) affected the attribution to a specific depth of the flux measurements and gas collection. In October 2014, a gas sample (MED 1) with very high gas flux was measured and collected 1 km west of the TCM site. This new emission suddenly appeared during a CPT (cone penetration test) in an area where spontaneous gas seepages and phenomena of surface heating were not previously recorded.

Gas sampling was carried out using a preevacuated 150 mL flask, for both chemical and isotopic ($\delta^{13}C$-CO_2 and $\delta^{13}C$-CH_4) analyses. Inorganic gases and CH_4 were analyzed with a Shimadzu 15A gas chromatographic system equipped with a 9 m long molecular sieve column and thermal conductivity detector. The analytical error was $<5\%$.

The $^{13}C/^{12}C$-CO_2 values (expressed as $\delta^{13}C$-CO_2 Vienna Peedee Belemnite (VPDB) ‰) were analyzed by mass spectrometry (Finningan Delta S), after a two-step extraction and purification procedures of the gas mixtures by using liquid N_2 and a solid-liquid mixture of liquid N_2 and trichloroethylene. Internal (Carrara and San Vincenzo marbles) and international (National Bureau of Standards (NBS) 18 and NBS 19) standards were used to estimate external precision. The analytical uncertainty and the reproducibility were ±0.05‰ and ±0.1‰, respectively. The $^{13}C/^{12}C$-CH_4 values (expressed as $\delta^{13}C$-CH_4 VPDB ‰) were determined by mass spectrometry (Varian MAT 250) at International Organization for Standardization 4 laboratories according to the procedure reported by *Stump and Frazer* [1973] and *Schoell* [1980]. The analytical uncertainty was ±0.15‰.

4. Results

4.1. Microseepage of CH_4 and CO_2

Preliminary data analysis involved the calculation of standard statistical parameters to evaluate the basic features of the CH_4 and CO_2 flux data. Due to their lognormal distribution, the experimental data were rearranged by logarithmic transformation of the original emission rate. The CH_4 and CO_2 soil flux thematic maps were built by using the kriging interpolation method [e.g., *Bergfeld et al.*, 2001], and for this stochastic simulation, a Gaussian model was derived from the empirical semivariogram. Each estimated logarithm value was then backtransformed in computer worksheet format by extracting the emission rate estimated for each grid point. After identifying threshold values, the total emission rate was calculated according to the method suggested by *Chiodini and Frondini* [2001]. The threshold values were defined by using the graphic method of *Sinclair* [1991]. The normal probability plots defined two populations for CO_2 (Figure 5a) and three for CH_4 (Figure 5b) fluxes. The intersection points allowed recognition of the threshold values (10 and 30 $g \times m^{-2} \times d^{-1}$, for CH_4 and CO_2, respectively) used for the calculation of the emission rates.

Descriptive statistical parameters and outputs ($t \times d^{-1}$) of the CO_2 and CH_4 emission rates (in $g \times m^{-2} \times d^{-1}$) measured in 2008 and 2013 and soil temperatures (measured at 77 sites in 2013) are reported in Table 1. Maps with the statistical interpolations of the CO_2 and CH_4 soil fluxes measured in 2008 and 2013 and temperatures measured in 2013 are reported in Figures 6a–6d and Figure 7.

In 2008, the CO_2 flux ranged from 0 to 139 $g \times m^{-2} \times d^{-1}$ with a mean value of 25.1 $g \times m^{-2} \times d^{-1}$, whereas those of CH_4 were from 0 to 51.8 $g \times m^{-2} \times d^{-1}$ with a mean value of 6.6 $g \times m^{-2} \times d^{-1}$. The anomalously high CO_2 and CH_4 fluxes (>30 and >10 $g \times m^{-2} \times d^{-1}$, respectively) were measured in two small ($<23{,}000$ m^2) sites located in the southwestern border of the study area (Figures 6a and 6b). In 2013, about 1 year after the May–June 2012 seismic event, the CO_2 fluxes ranged from 0.8 to 1180 $g \times m^{-2} \times d^{-1}$ with a mean

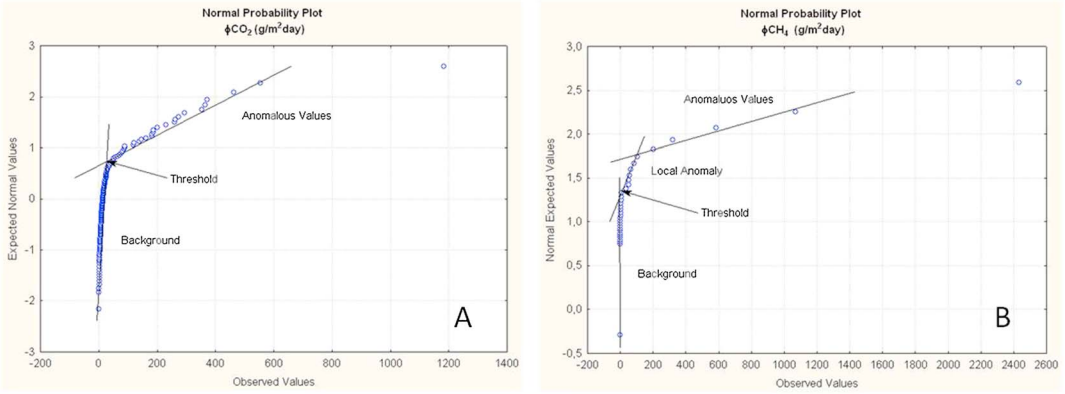

Figure 5. (a and b) The normal probability plot of the CO_2 and CH_4 fluxes for the 2013 survey, respectively.

value of 61.3 $g \times m^{-2} \times d^{-1}$, ~50% of them being higher than those typically measured for a mature soil (15 $g \times m^{-2} \times d^{-1}$ [*Capaccioni et al.*, 2011]).

Conversely, 92% of the measured CH_4 fluxes remained mostly below the detection limit ($<0.016\ g \times m^{-2} \times d^{-1}$), although in few sites, CH_4 fluxes largely higher than those of CO_2 were measured (up to 2430 $g \times m^{-2} \times d^{-1}$) (Figures 6c and 6d). Thus, the CO_2 and CH_4 maximum fluxes measured in 2013 significantly increased with respect to those of 2008, and the zone characterized by anomalous soil CO_2 fluxes extending eastward reached values up to ~38,000 m^2 (Table 1 and Figures 6a–6d). Accordingly, the total CO_2 and CH_4 emissions from the whole area increased by more than 1 order of magnitude, passing from 0.33 to 3.94 and from 0.17 to 1.93 $t \times d^{-1}$, respectively (Table 1). Soil temperatures, measured at 30 cm depth, showed a positive correlation with CO_2 ($r^2 = 0.69$), whereas no significant correlation with the CH_4 fluxes was observed (Figures 7 and 8, respectively).

Table 1. Descriptive Statistics of CO_2 and CH_4 Fluxes, Total Output, and Soil Temperature Measured in the Study Site Area

	Population	Value Range	Mean	Median	Standard Deviation	Area (m^2)
		ϕCO_2 ($g \times m^{-2} \times d^{-1}$)				
2008 data	overall population	0–139	25.1	7.6	46.0	258,720
	Bg	0–30	7.1	7.3	2.7	236,155
	1	30–100	0.0	0.0	0.0	20,059
	2	>100	134.0	134.0	7.1	2,506
		Output = 0.33 $t \times d^{-1}$ = 471.85 $t \times yr^{-1} \times km^{-2}$				
2013 data	overall population	0.8–1,184	61.3	15.0	135.5	258,720
	Bg	<30	11.7	9.7	7.7	220,021
	1	30–100	61.6	54.6	20.2	28,697
	2	100–210	163.0	216.9	29.6	7,018
	3	210–800	343.0	324.0	102.0	2,980
	4	>800	1184.0	1184.0	-	4
	soil *T* (°C)	21.7–44.1	27.5	25.6	5.7	-
		Output = 3.9 $t \times d^{-1}$ = 5,555 $t \times yr^{-1} \times km^{-2}$				
		ϕCH_4 ($g \times m^{-2} \times d^{-1}$)				
2008 data	overall population	0–51.8	6.6	0.0	15.9	258,720
	Bg	0–10	0.5	0.0	1.1	240,184
	1	10–30	0.0	0.0	0.0	14,559
	2	>30	43.1	43.1	12.3	3,977
		Output = 0.2 $t \times d^{-1}$ = 241.6 $t \times yr^{-1} \times km^{-2}$				
2013 data	overall population	0–2,432	37.0	0.0	232.0	258,720
	Bg	0–10	0.3	0.0	1.2	243,697
	1	10–30	0.0	0.0	0.0	4,719
	2	30–210	81.8	60.2	53.1	7,525
	3	210–1,000	454.0	454.0	186.0	2,740
	4	>1,000	1751.0	1751.0	963.0	39
		Output = 1.9 $t \times d^{-1}$ = 2717.9 $t \times yr^{-1} \times km^{-2}$				

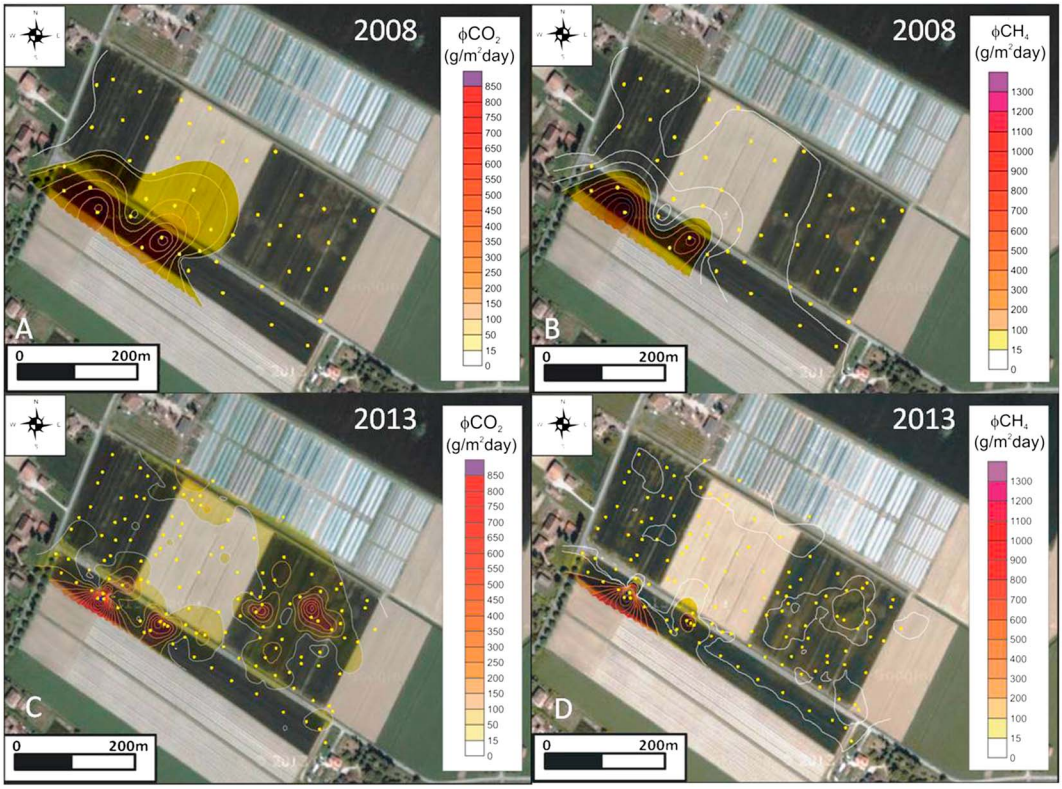

Figure 6. Contour maps of soil fluxes at the study site area: (a) CO_2 flux in 2008, (b) CH_4 flux in 2008, (c) CO_2 flux in 2013, and (d) CH_4 flux in 2013. The spatial distribution of the soil flux was computed by using the kriging estimation method. The location of measurement points are reported with yellow dots.

4.2. Physico-Chemical Parameters and Isotopic Data

The chemical and isotopic data of the soil gases collected during drilling of the 2.5 m deep piezometer are reported in Table 2 and plotted in Figure 9. The soil temperatures ranged from 36.4°C at the surface to 17.0°C at the bottom of the piezometer (−2.50 m), with a maximum measured temperature of 42.2°C at a depth of 0.6 m.

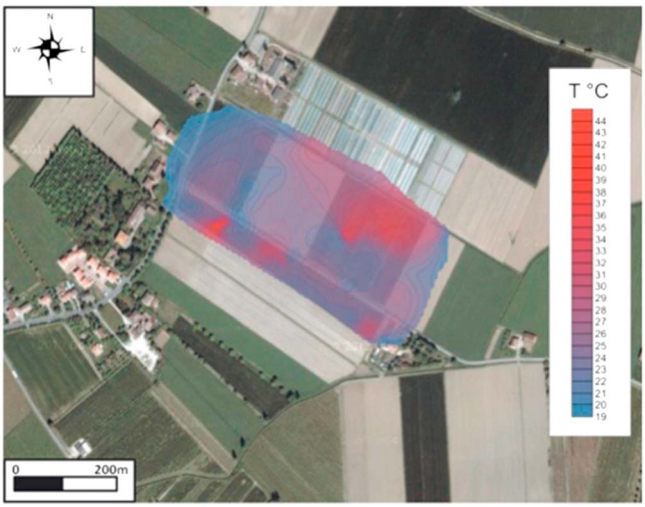

Figure 7. Contour maps of soil temperature at the study site area. Soil temperature was measured with a thermocouple at a depth of 0.30 m.

Within the first 20 cm, the temperature increased from 36.4 to 38.1°C. In this very shallow interval, the gas composition mainly consisted of atmospheric gases, with minor, though significant, amounts of CO_2 (up to 4.5 vol %), while CH_4 contents (<0.001 vol %) were negligible. At greater depth (0.30–0.70 m interval; Figure 9), the temperature reached its maximum value (42.2°C). Within this interval, the gas phase showed the highest CO_2 and the lowest O_2/N_2 ratio. The CO_2 contents reached a maximum of 17.1% at 30 cm depth, decreasing down to 6.9% at 0.70 cm depth. In the same interval, CH_4 passed from 0.34% to 51.0%, whereas a minimum value of 0.75% up to

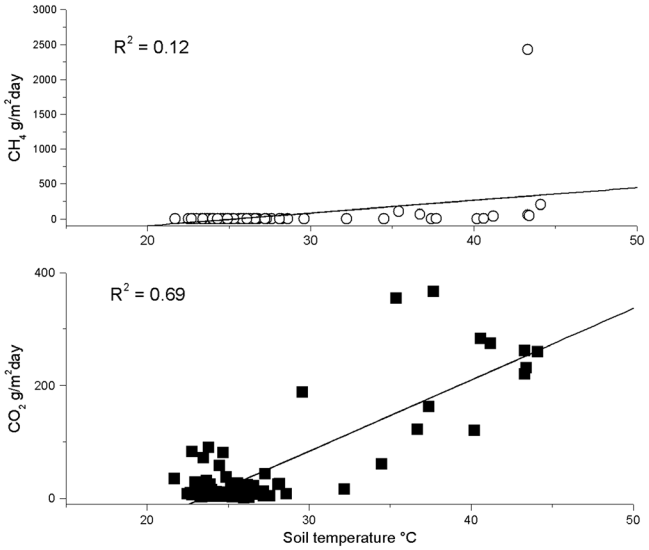

Figure 8. Soil temperatures collected at 30 cm depth versus CO_2 and CH_4 soil fluxes measured in the investigated area. The trend lines and the r^2 coefficients are also reported.

6.13% was recorded for O_2. As reported in Figure 9, in the 0.30–0.70 m interval, the O_2/N_2 decreases very rapidly from the atmospheric value (0.26) down to 0.009 at 0.5 m. From 0.70 to 2.50 m depth, the CH_4 contents showed no significant variations (~30%), whereas those of CO_2 were as low as 1.2%. The vertical profiles of the CO_2 flux (Table 2) displayed the maximum values within the interval of 0.50–0.80 m, where a relatively pervious loamy sandy layer was found (Figure 3). This suggests a control on gas flux exerted by the local permeability, whereas CH_4 flux steadily decreased from the maximum value at 2.5 m up to negligible values ($<0.002\ g \times d^{-1}$) at <0.30 m depth. In Figure 10, the vertical variability of the measured CO_2/CH_4 flux ratio is plotted. Within the 0.6–2.5 m interval, the CO_2/CH_4 flux ratio was $\ll 1$, whereas at <0.60 m depth, the CO_2/CH_4 flux ratio rapidly increased up to 2000 (at ~0.20 m depth).

The δ^{13}C-CH_4 and δ^{13}C-CO_2 values in the gases collected from the piezometer ranged from −72.3‰ to −62.5‰ and from −67.8‰ to −49.9‰ versus VPDB, respectively. The δ^{13}C-CH_4 displayed a vertical variability with the lowest values (<−68‰ versus VPDB) measured at >0.70 m depth and the highest ones (>−63.4‰ versus VPDB) at shallower depths. The δ^{13}C-CO_2 values showed an opposite behavior as the more positive values (>−65‰ versus VPDB) were measured at >0.70 m depths and the more negative (<−65‰ versus VPDB) were recorded at shallower depths. A striking "carbon isotopic inversion" between CH_4 and CO_2 (Figure 9) was recorded at depths <0.70 m, where the carbon isotopic signature of CO_2 was significantly lighter than that of CH_4.

The MED 1 gas sample (Figure 1b and Table 2) was also a CH_4-dominated gas emission, although characterized by higher flux ($13.45\ g \times d^{-1}$) and CH_4 contents (75.69 vol %) with respect to the TCM gases. The O_2/N_2 ratio was in good agreement with that of the atmosphere (i.e., no oxygen consumption), while the δ^{13}C-CH_4 and δ^{13}C-CO_2 values were −78.0 and −23.2‰, respectively.

5. Discussion

According to the geochemical and isotopic data, the gas seepage in the TCM area is characterized by the uprising of a N_2- and CH_4-dominated gas mixture with minor amounts of CO_2 and O_2. The N_2/Ar ratio is slightly higher (82 ÷ 89) with respect to that of the atmospheric gases (≈78), whereas O_2/N_2 is mostly lower. This suggests a minor addition of nonatmospheric N_2 (possibly organic) coupled with O_2 consumption likely caused by oxidation processes. A first arising question concerns how and where CH_4 is actually produced. As reported above, the TCM site is on top of the *Dorsale Ferrarese* tectonic fold located at <100 m depth below the alluvial cover (Figure 2a). Inspection of the subsoil stratigraphy has revealed the occurrence of gas and salty water seeps at depths ranging between 750 and 2000 ÷ 2300 m. At ≈2000 m depth, the prevailing stratigraphic unit consists of upper Miocene marls and organic-rich clays. Above this depth, methanogenic organic-rich layers of significant thickness were not recognized in the stratigraphic sequence (Figure 4). The measured thermal gradient in the area is quite low (1°C/100 m; Regione Emilia-Romagna (ER) report), with temperature not significantly exceeding 50°C at 2000 m depth. CH_4 can be produced and stored beneath the thrust surfaces from which it migrates upward along minor fault planes. As CH_4 rises up, it can also be stored within pervious horizons at shallower levels (such as the

Table 2. Depth, Temperature, CO_2, and CH_4 Fluxes (and Relative Ratios) From the Piezometer Expressed as Weight ($g \times d^{-1}$) and Volume ($L_{STP}\ d^{-1}$; STP: Standard Temperature and Pressure) per Day (See Text for Further Explanations) and Chemical Composition (in vol %), CO_2/CH_4 Ratio, and Carbon Isotopic Composition (in VPDB ‰) of the Gases Collected From the 2.5 m Deep Piezometer Each 10 cm Down to 80 cm Depth and Each 50 cm at Greater Depth[a]

ID	Depth (cm)	T (°C)	CO_2 (g/d)	CH_4 (g/d)	$\phi CO_2/\phi CH_4$	L_{STP}/d CO_2	L_{STP}/d CH_4	CO_2 % vv	CH_4 % vv	CO_2/CH_4 W/W	N_2 % vv	O_2 % vv	Ar % vv	O_2/N_2 V/V	$\delta^{13}C_{CH_4}$ PDB ‰	$\delta^{13}C_{CO_2}$ PDB ‰	$\delta^{13}C_{CH_4}$ PDB ‰	$\delta^{13}C_{CO_2}$ PDB ‰
0	0	36.4	0.203	0.000	1970.87	0.103	0.000				78.1	19.69	0.95	0.256				
1	10	36.7	0.131	0.000	276.37	0.067	0.001	1.26			79.46	15.05	0.97	0.252			−55.26	−65.91
2	20	38.1	0.191	0.000	1104.05	0.097	0.000	4.52			77.55	4.04	0.94	0.189	−63.21	−65.24		
3	30	38.5	0.189	0.002	102.58	0.096	0.003	17.14	0.328	143.70	82.93	1.22	0.93	0.052	−62.50	−66.71	−65.33	−66.75
4	40	38.1	0.275	0.009	29.53	0.140	0.013	13.99	0.93	41.37	81.78	0.75	0.95	0.015	−63.42	−67.71		
5	50	39.8	0.317	0.027	11.64	0.161	0.038	14.14	2.385	16.30	63.31	2.27	0.75	0.009	−63.37	−67.83	−70.83	−46.35
6	60	42.2	0.425	0.653	0.65	0.216	0.915	8.38	25.29	0.91	35.09	6.13	0.4	0.036	−68.97	−65.91		
7	70	38.4	0.314	1.191	0.26	0.160	1.669	6.91	51.47	0.37	54.44	5.86	0.64	0.175	−71.15	−55.21		
8	80	34.6	0.518	1.109	0.47	0.264	1.553	7.51	31.55	0.65	55.89	4.15	0.65	0.108	−71.73	−61.36		
10	100	31.6	0.484	0.982	0.49	0.247	1.376	4.09	35.22	0.32	60.55	2.07	0.7	0.074	−68.72	−49.86		
11	150	28.1	0.315	1.053	0.30	0.160	1.475	4.85	31.83	0.42	64.06	1.55	0.75	0.034	−72.31	−52.47		
12	200	21.5	0.342	1.510	0.23	0.174	2.115	3.48	30.16	0.32	63.62	2.87	0.73	0.024				
13	250	17.0	0.232	3.137	0.07	0.118	4.395	1.19	31.59	0.10	17.43	4.54	0.29	0.045				
MED 1		14.0	0.640	13.45	0.05	0.326	18.836	1.99	75.69	0.07				0.260	−78.00	−23.19		

[a]MED 1 is a gas sample that suddenly appeared during a CPT on mid-October 2014 at ~1 km west of TCM.

sandy river-channel facies, possibly referred to the Po riverbed). Depending on the cover permeability, its thickness and the possible occurrence of diffuse fracture networks CH_4 can reach the surface, such as at TCM site.

The origin of CH_4 in natural environments is mainly related to (i) microbial activity (methanogenic archaea) and (ii) thermogenic degradation of preexisting organic matter. These two different CH_4 sources produce distinct $^{13}C/^{12}C$ ratios: (1) thermogenic CH_4 typically shows $\delta^{13}C$ values ranging from −50 to −30‰ versus VPDB and (2) microbial CH_4 commonly has $\delta^{13}C$ values <-50‰ versus VPDB [e.g., *Schoell*, 1980, 1988; *Whiticar*, 1999; *McCollom and Seewald*, 2007]. The $\delta^{13}C$-CH_4 values measured in the gas samples collected during drilling were <-70‰ versus VPDB, therefore suggesting a prevailing microbial origin of CH_4. As reported above, a source located at 2000 m depth should be at a temperature of ≈50°C, which is within the typical range for biogenic production of CH_4 [*Valentine et al.*, 2004]. *Galand et al.* [2010] showed that bacterial methanogenesis in peatland ecosystems produces a carbon isotopic fractionation between CH_4 and the coexisting CO_2 of 41‰ to 72‰. *Whiticar* [1999] suggested a larger carbon isotopic fractionation ranging from 49 to 95‰ depending on (i) temperature [*Whiticar et al.*, 1986; *Hornibrook et al.*, 1997], (ii) isotope composition of precursor organic substrate, and (iii) rate of methanogenesis [*Zyakun*, 1992]. The experimental results of *Valentine et al.* [2004] indicated that CH_4 production due to bacterial CO_2 reduction causes a carbon isotope fractionation of 22–58‰. The isotopic difference (expressed as ($\Delta_{CO2\text{-}CH4}$) between the $\delta^{13}C$-CO_2 and $\delta^{13}C$-CH_4 values measured at TCM ranged from 20‰ at >0.50–0.60 m depths to −4.5‰ at shallower levels. Even when the highest recorded value ($\Delta_{CO2\text{-}CH4} = 20$‰) is considered, the isotopic fractionation between CH_4 and the coexisting CO_2 cannot be related to fractionation processes due to bacterial methanogenesis at depth. The achievement of isotopic equilibrium between these two carbon species can also be ruled out, since temperatures higher than 350°C would be required [*Giggenbach*, 1997]. Moreover, the

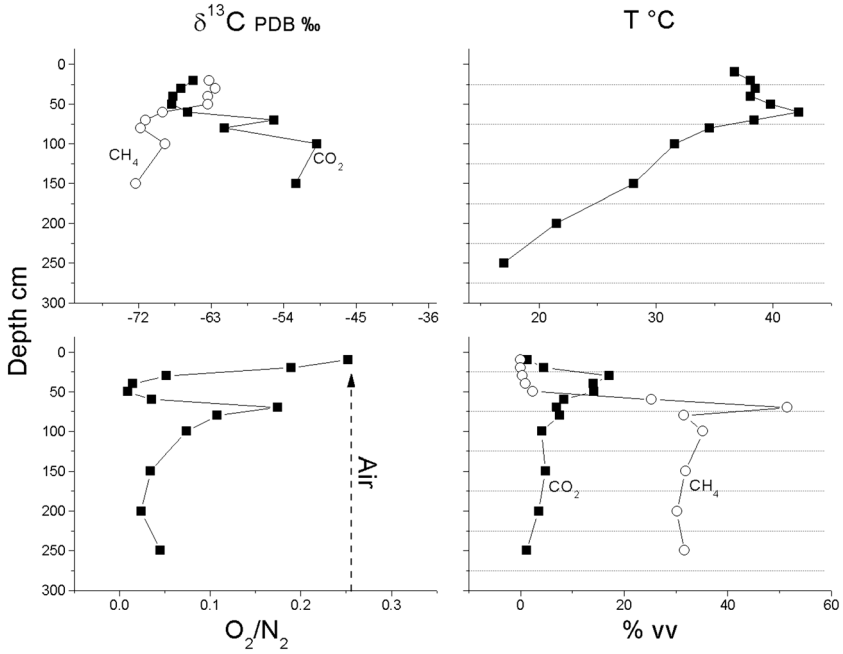

Figure 9. Vertical profiles of temperature and chemical and isotopic parameters on gases collected each 10 cm down to 80 cm depth and each 50 cm at greater depth.

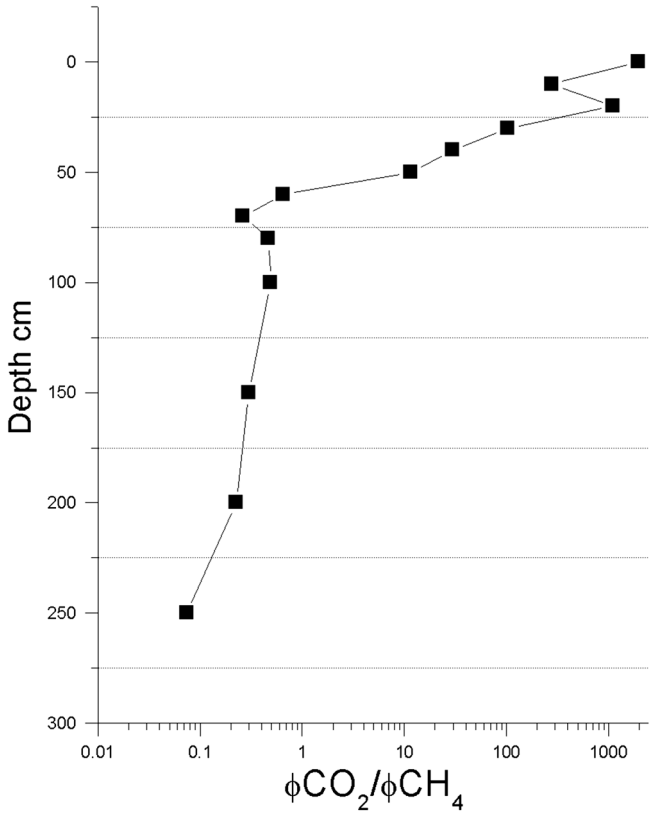

Figure 10. Vertical profiles of CO_2/CH_4 flux ratio measured during drilling of the piezometer. The respective measurements were carried out at depth intervals of 10 cm down to 80 cm depth and at intervals of 50 cm at greater depth. The strong increase of CO_2/CH_4 flux ratio at depth $<$50 cm appears meaningful.

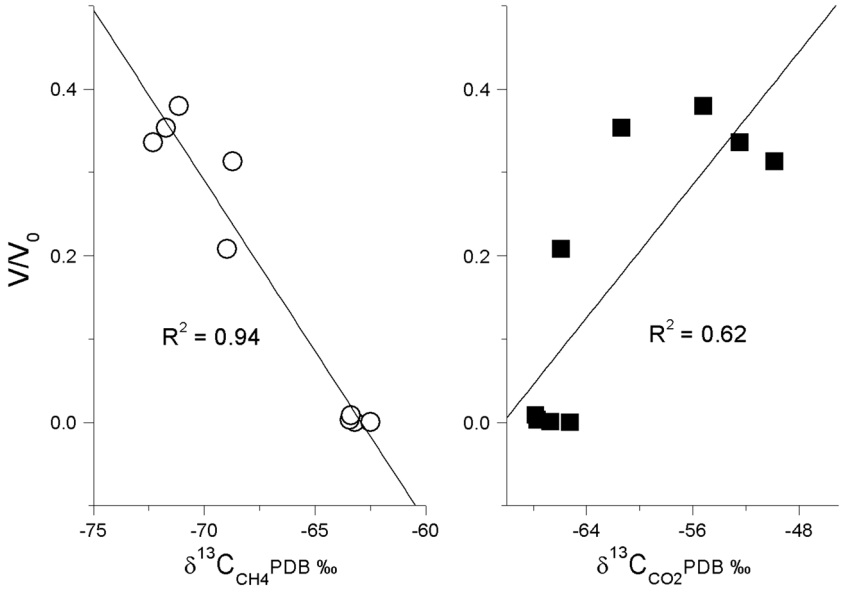

Figure 11. Residual volumetric fraction of CH_4 (see text for further explanation) of the gas phase collected each 10 cm down to 80 cm depth and each 50 cm at greater depth versus the measured δ^{13}C-CO_2 and δ^{13}C-CH_4 values. The trend lines and the r^2 coefficients are also reported.

composition of the gas sample (MED 1; Table 2), collected from a gas vent that suddenly appeared during a CPT ~1.0 km W of TCM, i.e., in an area previously free of both CH_4 seepages and anomalously high soil temperatures, is of particular interest. The chemical composition of MED 1 and TCM gases were similar such as their δ^{13}C-CH_4 values (−78.0‰). Vice versa, a strikingly different δ^{13}C-CO_2 value was measured in the MED 1 gas sample since it was significantly more positive (−23.2‰) than those measured at TCM. Both δ^{13}C-CH_4 (−78.0‰) and the $\Delta_{CO2\text{-}CH4}$ (54.8‰) value of MED 1 is in good agreement with that expected for bacterial methanogenesis [*Whiticar*, 1999; *Valentine et al*., 2004; *Galand et al*., 2010].

Dunfield et al. [2007] observed that CH_4 concentrations at Tikitere (New Zealand), a geothermal area with diffuse CH_4-rich gas emissions, reached the lowest contents near the surface (0.10–0.20 m depth) due to oxidative CH_4 consumption by methanotrophic bacteria. A similar condition was also observed at the TCM site, where the CH_4 contents became negligible at very shallow depth (<0.6 m), whereas those of CO_2 reached the relative highest concentrations. Moreover, at <0.60 m depth, the δ^{13}C-CO_2 values were more negative (~−68‰ versus VPDB) than those of δ^{13}C-CH_4 (~−63‰). This was not recorded at >0.50–0.60 m depths, where δ^{13}C-CO_2 ranged from −50 to −61‰ versus VPDB and δ^{13}C-CH_4 from −68.7 to −72‰ versus VPDB (Figure 9).

The gradual depletion of ^{13}C in CO_2 at shallower depth is consistent with a ^{13}C/^{12}C kinetic fractionation due to a partial $CH_4 \rightarrow CO_2$ conversion. $^{12}CH_4$ is indeed oxidized slightly faster than $^{13}CH_4$ [*Barker and Fritz*, 1981], and therefore, the CH_4-derived CO_2 can significantly be enriched in ^{12}C with respect to the residual CH_4. The residual volumetric fraction of CH_4, i.e., the ratio between the volumetric CH_4 fluxes measured at different levels (Table 2) and the maximum recorded volumetric CH_4 flux measured at the bottom of the piezometer (4.395 $L_{stp}\,d^{-1}$; Table 2), shows an inverse relation with the δ^{13}C-CH_4 values, whereas it is directly related to those of δ^{13}C-CO_2 (Figure 11). This behavior confirms the effect of the $CH_4 \rightarrow CO_2$ conversion, which likely derives by isotopic fractionation processes during oxidative consumption of CH_4 at decreasing depths. This produces isotopically light CO_2 and, consequently, ^{13}C-rich residual CH_4. In this context, the MED 1 emission may represent the pristine CO_2 and CH_4 isotopic compositions, likely before the growth of methane-utilizing bacteria (methanotrophs), whose metabolic activity promotes the CH_4 oxidation at shallow levels.

Summarizing, the measured carbon isotopic signature of CH_4 and CO_2 at TCM site is the result of the sequential combination of two processes:

1. Bacterial methanogenesis at depth (>2000 m), producing isotopically light CH_4 (δ^{13}C-$CH_4 = -78.0‰$) and relatively heavy CO_2 (δ^{13}C-$CO_2 = -23.2‰$);
2. Bacterial oxidation of CH_4 mainly within the most aerated loamy sandy layer located at very shallow depth, where isotopically lighter CO_2 (up to a δ^{13}C-$CO_2 = -67.8‰$) and heavier CH_4 (up to δ^{13}C-$CH_4 = -62.5‰$) are produced.

The fraction of the ^{12}C-rich CO_2 systematically increases upward due to the increasing CO_2 contribution from CH_4 oxidation.

At TCM, the observed anomalous ground temperature, as well as the relatively high CO_2 and CH_4 soil fluxes, cannot be referred to neither an anomalous thermal flux nor uprising hot fluids. As previously described, this area is indeed an alluvial plain with a normal-to-low geothermal gradient (1°C/100 m; Emilia-Romagna Region [*CNR*, 1982]), and the documented deep groundwater has a temperature not exceeding 21°C at 500 m. In 2013, the maximum ground temperature (44.1°C) was recorded in the SW limit of the investigated area (Figure 7), in correspondence with the highest CO_2 and CH_4 soil fluxes (350 and 2428 $g \times m^{-2} \times d^{-1}$, respectively; Figures 6c and 6d). As reported above, the spatial distribution of ground temperature is better related to the CO_2 flux than to that of CH_4. The spatial distribution of CH_4 fluxes appears to be characterized by few spots with very high fluxes (up to 2428 $g \times m^{-2} \times d^{-1}$), whereas most data were below the detection limit. A similar condition was observed for biogas microseepage from the Municipal Solid Waste Landfill [*Capaccioni et al.*, 2011]. In these anthropogenic systems, biogenic CH_4 was completely removed by microbial activity within the soil cover in sites where the biogas fluxes (mainly consisting of CO_2 and CH_4) were $<$20–30 $g \times m^{-2} \times d^{-1}$ [e.g., *Tassi et al.*, 2009]. Methane consumption progressively decreases as the CH_4 fluxes increase, likely due to kinetic effects. When biogas fluxes are $>$1000 $g \times m^{-2} \times d^{-1}$, CH_4 is not significantly removed within the soil cover [*Capaccioni et al.*, 2011]. At TCM, the maximum soil temperature (42.2°C) was recorded at 0.60 m depth, which corresponds to the maximum removal of CH_4 and O_2 and the highest CO_2 production, i.e., to the level of maximum efficiency of the $CH_4 \rightarrow CO_2$ conversion. In this context, the diffuse CO_2 seep is mainly the product of CH_4 oxidation at very shallow levels. Given the exothermic nature of the conversion process (800 $kJ \times mol^{-1}$ [*Ioannides and Verykios*, 1997]), this appears as the only plausible mechanism able to cause the measured soil heating at TCM. This explains (i) the correlation between the spatial distribution of soil temperature and CO_2 fluxes and (ii) the absence of soil CH_4 flux, since its values are slightly above than the detection limit. Conversely, CH_4 is detected at surface only when its flux is sufficiently high to avoid the complete conversion to CO_2. The produced H_2O surplus could be responsible for the gleying process that exclusively characterizes the shallow sediments where the $CH_4 \rightarrow CO_2$ conversion occurs.

6. Conclusions

At TCM, (i) soil temperature profile, (ii) compositional vertical patterns measured along the piezometer (Figure 9), and (iii) presence of metanotrophic bacteria in a soil sample collected at ~0.5–0.6 m depth (S. Fedi, personal communication) suggest the occurrence of exothermic, oxidative CH_4 removal as the main mechanism of soil heating at TCM. Oxidation of CH_4 is a highly exothermic process since 800 $kJ \times mol^{-1}$ (CH_4) [*Ioannides and Verykios*, 1997] is produced. Methane oxidation can only occur in an aerobic environment [*Lerner et al.*, 2000]. It is difficult to verify whether oxidation and heating only occur in correspondence of a specific layer or spread throughout all the soil thickness. Nevertheless, it can be assessed that the $CH_4 \rightarrow CO_2$ conversion achieved the highest efficiency close to the loamy sandy layer, which is the relatively more permeable and aerated strata within the studied soil profile.

The numerical simulation carried out by *Nespoli et al.* [2015] provides a good fitting between observed and simulated temperature profiles. It describes heat generation due to CH_4 oxidation within an unsaturated soil. The heat source is placed inside the more pervious layer at 0.6 and 0.7 m depths. Here CH_4 oxidation takes place, and the heat production is depending on the CH_4 flux. Numerical simulations consider different CH_4 fluxes, explore the efficiency of the process of CH_4 oxidation (producing different rates of heat generation), and take into account the seasonal effects.

According to the experimental results of *Whalen et al.* [1990], the kinetic constant of CH_4 oxidation, rather than the type of the microbial communities, depends on CH_4 concentration, temperature, and content of

the soil moisture. *Sundh et al.* [1995] described some parameters able to control the aerobic methane oxidation, as follows: *…the greater the vertical extension of aerated surface peat, the higher the methane oxidation capacity. ….These results suggest that the supplies of methane and oxygen largely control the biomass of methanotrophs across plant communities.* This implies that changes in the groundwater table level (and hence in the supply of CH_4 and O_2 to the methanotrophs) could strongly affect the in situ oxidation rates and cause large temporal variation of the oxidized CH_4 fraction and, consequently, the amount of heat released by the exothermic reaction. The previously cited evidence provide a very shallow and local source for the anomalous heating at TCM related to the presence of CH_4 microseepage and oxidation at shallow soil levels due to methanotrophic bacteria.

According to *Bonori et al.* [2000] and *Cremonini* [2010], data on seismic profiles highlight the diffuse presence of uprising fluids, likely consisting of biogenic methane generated by bacterial degradation of organic matter at depth. Earthquakes may increase fluid propagation toward the surface by increasing both the pore pressure and/or opening new fractures that favor an increasing permeability. Despite the fact that only two CH_4 and CO_2 isoflux maps (2008 and 2013; Figure 6) are clearly not enough to identify any flux increase associated with the May–June 2012 Emilia earthquake, they nevertheless suggest that in the TCM area, the CH_4 and CO_2 fluxes have significantly changed in time and space and this variability should be investigated in more detail in the next future. Therefore, although direct relationships between gas fluxes, soil temperature, and the earthquake events of 2012 in the area cannot be definitively established, we can speculate that a possible increase of the CH_4 fluxes from depth may have caused a diffuse temperature increase of soil and shallow aquifers due to superficial $CH_4 \rightarrow CO_2$ conversion. In our opinion, this mechanism may also explain the sudden and spontaneous phenomena, such as bubbling waters, heated soils and, occasionally, heated waters, reported by several witnesses in the area during and after the seismic sequence of the May–June 2012 Emilia earthquake. In a recent study, *Qin et al.* [2012] reported a series of preliminary data about the occurrence of a preseismic and coseismic thermal anomalies in the area revealed by satellite on 12 May 2012, i.e., 8 days before the 20 May 2012 earthquake (M_L 5.9) and on 24 May 2012, i.e., 5 days before the 29 May 2012 earthquake (M_L 5.8). These authors claimed for an increasing emission of greenhouse gases (CO_2 and CH_4) into the atmosphere from the ground, although according to the same authors, other possible heat sources such as the release of latent heat due to near-surface air ionization, stress-induced thermal effects due to friction, and uprising hot fluids could not be ruled out. In our opinion, a further heat source may be related to CH_4 oxidation processes at shallow levels. This implies that monitoring the occurrence of thermal anomalies in the Emilia region actually means to monitor the temporal evolution of CH_4 soil fluxes and the efficiency of its superficial oxidation. This aspect should be considered when monitoring surveys of seismic areas, such as those hit by the May–June 2012 events, are to be planned.

Acknowledgments
Many thanks are due to S. Venturi for her help during the soil gas sampling and to Alessandro Escher, the owner of the sampling area, and his assistant M. Masi., J. Lewicki, and another anonymous reviewer are gratefully acknowledged for their useful comments and suggestions in an early version of the manuscript. The whole data set of the CO_2 and CH_4 flux values is available upon request at bruno.capaccioni@unibo.it.

References

Amorosi, A., and M. L. Colalongo (2005), The linkage between alluvial and coeval nearshore marine successions: Evidence from the late Quaternary record of the Po river plain, Italy, in *Fluvial Sedimentology VII*, edited by M. D. Blum, S. B. Marriott, and S. F. Leclair, pp. 257–275, International Association of Sedimentologists, Blackwell, Oxford, U. K.

Amorosi, A., M. C. Centineo, and P. Severi (2000), Stratigrafia dei depositi tardoquaternari lungo la sezione Bologna-Valli di Comacchio (Pianura padana sud-orientale), in *Le Pianure: Conoscenza e Salvaguardia (Atti Convegno, Ferrara 1999)* [in Italian], edited by E. Romagna, pp. 311–314, Ufficio Geologico, Servizio -SIG Regione, Bologna, Italy.

Amorosi, A., M. Pavesi, M. Ricci Lucchi, G. Sarti, and A. Piccin (2008), Climatic signature of cyclic fluvial architecture from the Quaternary of the central Po Plain, Italy, *Sediment. Geol.*, *209*, 58–68.

Anzidei, M., A. Maramai, and P. Montone (Eds.) (2012), *The Emilia (Northern Italy) Seismic Sequence of May-June, 2012: Preliminary Data and Results*, Ann. Geophys., vol. 55, pp. 842, Bologna, Italy.

Barchi, M., A. Landuzzi, G. Minelli, and G. Pialli (2001), Outer northern Apennines, in *Anatomy of an Orogen: Northern Apennines and Adjacent Mediterranean Basins*, edited by G. B. Vai and I. P. Martini, pp. 215–254, Kluwer Acad., Dordrecht, Netherlands.

Barker, J. F., and P. Fritz (1981), Carbon isotope fractionation during microbial methane oxidation, *Nature*, *293*, 289–291.

Bergfeld, D., F. Goff, and C. J. Janik (2001), Elevated carbon dioxide flux at the Dixie Valley geothermal field, Nevada: Relations between surface phenomena and the geothermal reservoir, *Chem. Geol.*, *177*(1–2), 43–66.

Bianchini, G., S. Cremonini, D. Di Giuseppe, G. Vianello, and L. Vittori Antisari (2014), Multiproxy investigation of a Holocene sedimentary sequence near Ferrara (Italy): Clues on the physiographic evolution of the eastern Padanian plain, *J. Soils Sediments*, *14*, 230–242.

Boccaletti, M., and L. Martelli (2004), Carta sismo-tettonica della Regione Emilia-Romagna, scala 1:250.000 e note illustrative [in Italian], Selca, Firenze.

Bonori, O., et al. (2000), Geochemical and geophysical monitoring in tectonically active areas of the Po Valley (N. Italy). Case histories linked to gas emission structures, *Geogr. Fis. Din. Quat.*, *23*, 3–20.

Borgatti, L., A. E. Bracci, S. Cremonini, and G. Martinelli (2012), Searching for the effects of the May-June 2012 Emilia seismic sequence (northern Italy): Medium-depth deformation structures at the periphery of the epicentral area, *Ann. Geophys.*, *55*, 717–725.

Brombach, T., J. C. Hunziker, G. Chiodini, C. Cardellini, and L. Marini (2001), Soil diffuse degassing and thermal energy fluxes from the southern Lakki plain, Nisyros (Greece), *Geophys. Res. Lett.*, *28*, 69–72, doi:10.1029/2000GL008543.

Capaccioni, B., C. Caramiello, F. Tatàno, and A. Viscione (2011), Effects of a temporary HDPE cover on landfill gas emissions: Multiyear evaluation with the static chamber approach at an Italian landfill, *Waste Manage.*, *31*, 956–965.

Cardellini, C., G. Chiodini, F. Frondini, D. Granieri, J. Lewicki, and L. Peruzzi (2003), Accumulation chamber measurements of methane fluxes: Application to volcanic-geothermal areas and landfills, *Appl. Geochem.*, *18*, 45–54.

Carminati, E., D. Scrocca, and C. Doglioni (2010), Compaction-induced stress variations with depth in an active anticline: Northern Apennines, Italy, *J. Geophys. Res.*, *115*, B02401, doi:10.1029/2009JB006395.

Cerrina Feroni, A., L. Martelli, P. Martinelli, and G. Ottria (2002), Carta geologico-strutturale dell'Appennino emiliano-romagnolo in scala 1:250.000, Regione Emilia-Romagna C.N.R., Pisa, S.EL.CA., Firenze.

Cesca, S., T. Braun, F. Maccaferri, L. Passarelli, E. Rivalta, and T. Dahm (2013), Source modelling of the M5–6 Emilia–Romagna, Italy, earthquakes (2012 May 20–29), *Geophys. J. Int.*, *193*, 1658–1672, doi:10.1093/gji/ggt069.

Chiodini, G., and F. Frondini (2001), Carbon dioxide degassing from the Albani Hills volcanic region, central Italy, *Chem. Geol.*, *177*, 67–83.

Chiodini, G., F. Frondini, and B. Raco (1996), Diffuse emission of CO_2 from the Fossa crater, Vulcano Island (Italy), *Bull. Volcanol.*, *58*, 41–50.

Chiodini, G., R. Cioni, M. Guidi, B. Raco, and L. Marini (1998), Soil CO_2 flux measurements in volcanic and geothermal areas, *Appl. Geochem.*, *13*, 543–552.

Chiodini, G., R. Cioni, M. Guidi, G. Magro, L. Marini, C. Panichi, B. Raco, and M. Russo (2000), Geochemical monitoring of the Phlegrean fields and Vesuvius (Italy) in 1996, *Acta Vulcanol.*, *12*, 117–119.

Cicerone, R. J., and R. S. Oremland (1988), Biogeochemical aspects of atmospheric methane, *Global Biogeochem. Cycles*, *2*, 299–327, doi:10.1029/GB002i004p00299.

C.N.R. (1982), Caratteri geoidrologici e geotermici dell'Emilia-Romagna. Programmi e prospettive per lo sfruttamento delle risorse geotermiche regionali, Regione Emilia-Romagna e Consiglio Nazionale delle Ricerche, Collana di orientamenti geomorfologici ed agronomico-forestali [in Italian], 177 pp.

C.N.R. (1990), *Structural Model of Italy, 1:500.000, Foglio 1*, edited by G. Bigi et al., Selca, Firenze.

Cremonini, S. (1993), Alcuni dettagli fotografici per le ricostruzioni paleo ambientali nella Pianura Padana [in Italian], *Civiltà Padana*, *4*, 145–171.

Cremonini, S. (2007), Some remarks on the evolution of the Po river plain (Italy) over the last four millennia, in *China-Otaly Bilateral Symposium on the Coastal Zone: Evolution and Safeguard, Bologna, 4–8 November*, edited by F. Marabini, A. Galvani, and M. Ciabatti, pp. 17–24, Bologna, Italy.

Cremonini, S. (2010), A preliminary overview of sinkholes in the Emilia-Romagna Region (Italy), in *II Int. Workshop "I sinkholes, gli sProfondamenti Catastrofici Nell'ambiente Naturale ed in Quello aNtropizzato"*, pp. 257–281, ISPRA, Rome, 3–4 December 2009.

Dondi, L., F. Mostardini, and A. Rizzini (1982), Evoluzione sedimentaria e paleogeografia nella Pianura Padana, in *Guida alla Geologia del Margine Appenninico-Padano* [in Italian], Guida Geol. Reg., edited by G. Cremonini and F. Ricci Lucchi, pp. 47–58, Bologna, Italy.

Dunfield, P. F., et al. (2007), Methane oxidation by an extremely acidophilic bacterium of the phylum *Verrucomicrobia*, *Nature*, *450*, 879–882.

Etiope, G. (2009), Natural emissions of methane from geological seepage in Europe, *Atmos. Environ.*, *43*, 1430–1443.

Etiope, G., and R. W. Klusman (2002), Geologic emissions of methane to the atmosphere, *Chemosphere*, *49*, 777–778.

Etiope, G., T. Fridriksson, F. Italiano, W. Winiwarter, and J. Theloke (2007), Natural emissions of methane from geothermal and volcanic sources in Europe, *J. Volcanol. Geotherm. Res.*, *165*, 76–86, doi:10.1016/j.jvolgeores.2007.04.014.

Fantoni, R., and R. Franciosi (2010), Mesozoic extension and Cenozoic compression in Po Plain and Adriatic foreland, *Rend. Fis. Acc. Lincei*, *21*, 197–209.

Galand, P. E., K. Yrjala, and R. Conrad (2010), Stable carbon isotope fractionation during methanogenesis in three boreal peatland ecosystems, *Biogeosciences*, *7*, 3893–3900.

Galli, P., S. Castenetto, and E. Peronace (2012), The MCS macroseismic survey of the Emilia 2012 earthquakes, *Ann. Geophys.*, *55*, 663–672.

Gasperi, G., and M. Pellegrini (1981), in *Note di Geologia del Comprensorio della Bassa Pianura Modenese (Comuni di: Camposanto, Cavezzo, Concordia, Finale E., Medolla, S. Felice s.P., S. Possidonio, S. Prospero)* [in Italian], edited by M. Calzolari, Banca Popolare di Cavezzo, 107 pp.

Ghielmi, M., M. Minervini, C. Nini, S. Rogledi, M. Rossi, and A. Vignolo (2010), Sedimentary and tectonic evolution in the eastern Po-Plain and northern Adriatic Sea area from Messinian to middle Pleistocene (Italy), in *Nature and Geodynamics of the Northern Adriatic Lithostere*, Rend. Fis. Acc. Lincei, vol. 21/1, edited by F. P. Sassi, G. Dal Piaz, and C. Doglioni, pp. 131–166.

Giggenbach, W. F. (1997), Relative importance of thermodynamic and kinetic processes in governing the chemical and isotopic composition of carbon gases in high-heat flow sedimentary basins, *Geochim. Cosmochim. Acta*, *61*, 3763–3785.

Govoni, A., et al. (2014), The 2012 Emilia seismic sequence (northern Italy): Imaging the thrust system by accurate aftershock location, *Tectonophysics*, *622*, 44–65.

Hansen, J., M. Sato, A. Lacis, R. Ruedy, I. Tegen, and E. Mathews (1998), Climate forcing in the industrial era, *Proc. Natl. Acad. Sci. U.S.A.*, *95*, 12,753–12,758.

Hornibrook, E. R. C., F. J. Longstaffe, and W. S. Fyfe (1997), Spatial distribution of microbial methane production pathways in temperate zone wetland soils: Stable carbon and hydrogen isotopes evidence, *Geochim. Cosmochim. Acta*, *61*, 745–753.

International Commission on Hydrocarbon Exploration and Seismicity in the Emilia Region (ICHESE) (2014), Report on the hydrocarbon exploration and seismicity in Emilia region, International Commission on Hydrocarbon Exploration and Seismicity in the Emilia Region, 213 pp.

Ioannides, T., and X. E. Verykios (1997), Application of a dense silica membrane reactor in the reactions of dry reforming and partial oxidation of methane, *Catal. Lett.*, *36*, 165–169.

Kirschke, S., et al. (2013), Three decades of global methane sources and sinks, *Nat. Geosci.*, *6*, 813–823, doi:10.1038/ngeo1955.

Lelieveld, J., P. J. Crutzen, and F. J. Dentener (1998), Changing concentration, lifetime and climate forcing of atmospheric methane, *Tellus, Ser. B*, *50*, 128–150.

Lerner, D. D., S. F. Thornton, S. A. Banwart, S. Bottrell, J. J. Higgo, R. W. Pickup, H. E. Mallinson, M. Spence, and G. M. Williams (2000), Ineffective natural attenuation of degradable organic compounds in groundwater, *Groundwater*, *38*, 922–928.

McCollom, T. M., and J. S. Seewald (2007), Abiotic synthesis of organic compounds in deep-sea hydrothermal environments, *Chem. Rev.*, *107*, 382–401.

Michetti, A. M., et al. (2012), Active compressional tectonics, Quaternary capable faults, and the seismic landscape of the Po Plain [northern Italy], *Ann. Geophys.*, *55*, 969–1001.

Nardon, S., D. Marzorati, A. Bernasconi, S. Cornini, M. Gonfalini, S. Mosconi, A. Romano, and P. Terdich (1991), Fractured carbonate reservoir characterization and modeling a multidisciplinary case study from the Cavone oil field, Italy, *First Break*, *9*, 553–565.

Nespoli, M., M. Todesco, B. Capaccioni, and S. Cremonini (2015), Ground heating and methane oxidation processes at shallow depth in Terre Calde di Medolla (Italy): Numerical modeling, *J. Geophys.Res. Solid Earth*, *120*, doi:10.1002/2014JB011636.

Norman, J. M., R. Garcia, and S. B. Verma (1992), Soil surface CO_2 fluxes and the carbon budget of a grassland, *J. Geophys. Res.*, *97*, 18,845–18,853, doi:10.1029/92JD01348.
Norman, J. M., C. J. Kucharik, S. T. Gower, D. D. Baldocchi, P. M. Crill, M. Rayment, K. Savage, and R. G. Striegl (1997), A comparison of six methods for measuring soil–surface carbon dioxide fluxes, *J. Geophys. Res.*, *102*, 28,771–28,777, doi:10.1029/97JD01440.
Picotti, V., and F. J. Pazzaglia (2008), A new active tectonic model for the construction of the northern Apennines mountain front near Bologna (Italy), *J. Geophys. Res.*, *113*, B08412, doi:10.1029/2007JB005307.
Qin, K., L. X. Wu, A. De Santis, and G. Cianchini (2012), Preliminary analysis of surface temperature anomalies that preceded the two major Emilia 2012 earthquakes [Italy], *Ann. Geophys.*, *55*, 823–828.
Rogie, J. D., D. M. Kerrick, G. Chiodini, and F. Frondini (2000), Flux measurements of nonvolcanic CO_2 emission from some vents in central Italy, *J. Geophys. Res.*, *105*, 8435–8445, doi:10.1029/1999JB900430.
Schoell, M. (1980), The hydrogen and carbon isotopic composition of methane from natural gases of various origins, *Geochim. Cosmochim. Acta*, *44*, 649–661.
Schoell, M. (1988), Multiple origins of methane in the Earth, *Chem. Geol.*, *71*, 1–10.
Sciarra, A., B. Cantucci, M. Buttinelli, G. Galli, M. Nazzari, L. Pizzino, and F. Quatrocchi (2012), Soil-gas survey of liquefaction and collapsed caves during the Emilia seiemic sequence, *Ann. Geophys.*, *55*, 803–809.
Sciarra, A., D. Cinti, L. Pizzino, M. Procesi, N. Voltattorni, S. Mecozzi, and F. Quattrocchi (2013), Geochemistry of shallow aquifers and soil gas surveys in a feasibility study at the Rivara natural gas storage site [Po Plain, northern Italy], *Appl. Geochem.*, *34*, 3–22.
Scrocca, D., E. Carminati, C. Doglioni, and D. Marcantoni (2007), Slab retreat and active shortening along the central-northern Apennines, in *Thrust Belts and Foreland Basins: From Fold Kinematics To Hydrocarbon Systems*, Frontier in Earth Sciences, edited by O. Lacombe et al., pp. 471–487, Springer, London.
Sinclair, A. J. (1991), A fundamental approach to threshold estimation in exploration geochemistry: Probability plots revisited, *J. Geochem. Explor.*, *41*, 1–22.
Spinelli, A. G. (1893), Una salsa e terre calde in Medolla, Il Panaro–La Gazzetta di Modena, 87.
Spinelli, A. G., and A. Cuoghi Costantini (1893), Una salsa e terre calde in Medolla, Il Panaro–La Gazzetta di Modena, 117 pp.
Stump, R. K., and J. W. Frazer (1973), Simultaneous determination of carbon, hydrogen and nitrogen in organic compounds, *Rep. 1973*, UCID-16918, Univ. California, Livermore, Calif.
Sundh, I., C. Mikkelä, M. Nilsson, and B. H. Svensson (1995), Potential aerobic methane oxidation in a Sphagnum-dominated peatland controlling factors and relation to methane emission, *Soil Biol. Biochem.*, *27*, 829–837.
Tassi, F., G. Montegrossi, O. Vaselli, C. Liccioli, S. Moretti, and B. Nisi (2009), Degradation of C2-C15 volatile organic compounds in a landfill cover soil, *Sci. Total Environ.*, *407*, 4513–4525, doi:10.1016/j.scitotenv.2009.04.022.
Tassi, F., M. Bonini, G. Montegrossi, F. Capecchiacci, B. Capaccioni, and O. Vaselli (2012), Origin of light hydrocarbons in gases from mud volcanoes and CH_4-rich emissions, *Chem. Geol.*, *294–295*, 113–126.
Valentine, D. L., A. Chidthaisong, A. Rice, W. S. Reeburgh, and S. C. Tyler (2004), Carbon and hydrogen isotope fractionation by moderately thermophilic methanogens, *Geochim. Cosmochim. Acta*, *68*, 1571–1590.
Ventura, G., and R. Di Giovambattista (2013), Fluid pressure, stress field and propagation style of coalescing thrusts from the analysis of the 20 May 2012 M_L 5.9 Emilia earthquake (northern Apennines, Italy), *Terra Nova*, *25*, 72–78, doi:10.1111/ter.12007.
Whalen, S. C., W. S. Reeburgh, and K. A. Sandbeck (1990), Rapid methane oxidation in a landfill cover soil, *Appl. Environ. Microbiol.*, *56*, 3405–3411.
Whiticar, M. J. (1999), Carbon and hydrogen isotope systematics of bacterial formation and oxidation of methane, *Chem. Geol.*, *161*, 291–314.
Whiticar, M. J., E. Faber, and M. Schoell (1986), Biogenic methane formation in marine and freshwater environments: CO_2 reduction vs. acetate fermentation—Isotopic evidence, *Geochim. Cosmochim. Acta*, *50*, 693–709.
Zyakun, A. M. (1992), Isotopes and their possible use as biomarkers of microbial products, in *Bacterial Gas*, edited by R. Vially, pp. 27–46, Editions Technip, Paris.